Supplement for

Summertime photochemistry during CAREBeijing-2007: RO_x budgets and O_3 formation

Z. Liu[1*] Y. Wang[1] D. Gu[1] C. Zhao[1,] L. G. Huey[1] R. Stickel[1] J. Liao[1] M. Shao[2] T. Zhu[2] L. Zeng[2] A. Amoroso[3] F. Costabile[4] C.-C. Chang[5] and S.-C. Liu[5]**

[1]{School of Earth and Atmospheric Science, Georgia Institute of Technology, Atlanta, GA, USA}
[2]{College of Environmental Sciences and Engineering, Peking University, Beijing, China}
[3]{Institute for Atmospheric Pollution, National Research Council (CNR-IIA), Rome, Italy}
[4]{Institute for Atmospheric Sciences and Climate (ISAC), CNR, Rome, Italy}
[5]{Research Center for Environmental Changes (RCEC), Academic Sinica, Taipei, China}

[*] {Now at Combustion Research Facility, Sandia National Laboratories, Livermore, CA, USA}
[**]{Now at the Pacific Northwest National Laboratory, Richland, Washington, USA}

Correspondence to: Z. Liu (zhen.liu@eas.gatech.edu)

Descriptions of instruments and experimental methods

O_3 and CO measurements. O_3 and CO were measured with commercial instruments (ECOTECH, EC9810 and EC9830). The EC9810 Ozone Analyzer combines microprocessor control with ultraviolet (UV) photometry to measure O_3 with a detection limit of 0.5 ppbv. The EC9830 series of Carbon Monoxide analyzers use NDIR gas filter correlation photometry to measure Carbon Monoxide (CO). Zero signals were routinely measured every 2 hours by supplying dry purified air into the sample line. We note that as water vapor interferes the CO analyzer, using dry air will give lower baseline values, thus higher CO concentration. The uncertainties for these measurements are estimated to be 5% (1 standard deviation, and so for all other uncertainties).

NO and NO_y measurements. NO mixing ratios were measured with a custom chemiluminescence detector (*S1*). The instrument was calibrated periodically (2–4 hours) by a standard addition of a known amount of nitric oxide. Background levels were obtained periodically (30 minutes) by switching the sampled flow through a pre-reactor. NO_y levels were measured by use of a molybdenum converter operated at 300□. The sample flow to the NO detector was periodically switched between ambient and the converter by a three way Teflon valve. NO_y conversion levels were estimated to be greater than 97% for NO_2. The conversion efficiency for NO_2 were examined before and after the campaign and appears to be quantitative i.e. > 95%. The conversion efficiency for HNO_3 was found to be greater than 85% after the mission. We did not look at anything in Beijing during the measurements, as we didn't have the ability to do so. High conversion efficiency for PAN (greater than 95%) can be expected because PAN will decompose to NO_2 readily at high temperature. The efficiency for NO should be comparable with NO_2, too. Organic nitrates were probably close to 100% converted. The uncertainties for NO and NO_y measurements are estimated to be 5% and 10%, respectively.

PAN measurements. Peroxyacetyl nitrate (PAN) were measured using a chemical ionization mass spectrometer (CIMS) (*S2, S3*). The instrument was calibrated periodically with a photolytic PAN source and the background response of the instrument was determined by periodically scrubbing sampled air through hot stainless steel tubing (200 ^{o}C) (*S4*). The sensitivity of the instrument was found to decrease at high NO_x levels. High levels of NO can lead to a decrease in sensitivity to the CIMS PAN measurements. For the conditions in Beijing, 10 ppbv of NO decreased the PAN sensitivity by 10% with higher levels decreasing the sensitivity further. NO levels above 10 ppbv were observed 20% of the time but only at night. Consequently, there is essentially no correction for the impact of NO during the day on PAN sensitivity. The measurement uncertainty of PAN at night during high levels of variable NO is larger than during the day. Detection limit for PAN is 7 pptv for 1 second integration period and a signal to noise ratio of 3. The uncertainties for PAN measurements are estimated to be 10%.

HONO measurements. HONO was measured with a liquid coil scrubbing/UV–vis instrument (*S5, S6*). Briefly, gaseous HONO was trapped quantitatively in a 10-turn coil sampler using 1mm phosphate buffer. The scrubbing solution was then derivatized with sulfanilamine (SA)/N-(1-naphtyl)-ethylendiamine (NED), subsequently analyzed using high-performance liquid chromatography (HPLC), and detected by UV-vis absorption.

Interferences during sampling were studied in our laboratory in Rome (*S6*) and directly at Beijing using sodium carbonate denuders (*S7*). We used the denuder respectively in front of the Teflon tube and before the trap coils. The denuder in front of Teflon tube was used to study the possible formation of HONO from NO_2 and humidity on the tubing walls (*S8*), while the denuder before the inlet traps was used to study the nitrite formation in the water solution due to the reaction of $NO_3^- + SO_3 \rightarrow NO_2^- + SO_4^{2-}$. Under summer conditions at Beijing we observed interferences on the

order of 2–9% of the observed HONO mixing ratio. The inlet tube was 70 cm and the residence time of the air in the tube was less than 2 sec. The detection limit of the HONO instrument is less than 0.8 pptv. The uncertainty for HONO measurements (after removing known interference) is estimated to be 10%.

VOC measurements. C_3-C_9 NMHCs were continuously measured with 30 minute time resolution, using a combination of two online GC-FID/PID systems (Syntech Spectra GC-FID/PID GC955 series 600/ 800 VOC analyzer) (*S9*), one for the C_3–C_5 NMHCs, using a gas chromatograph with pre-concentration on Carbosieves SIII at 5 ^{o}C, followed by thermal desorption and separation on a capillary film column and a capillary PLOT column, and quantification by a photo ionization detector (PID) and a flame ionization detector (FID). The other system is for C_6–C_9 NMHCs analysis; air samples are pre-concentrated on Tenax GR at normal temperature, thermal desorbed, separated on an ATTM-1 column, and detected by a PID. For each analysis, an air sample with a volume of 250mL was sampled. Calibration was performed before and after the campaign by using a gas standard containing 39 target species with mixing ratios of 1ppm in nitrogen, prepared by the gravimetric method (Spectra gases, Restek Corporation, USA). The detection limits are estimated to be 10 to 90 pptv, and the uncertainty is estimated to be 5%.

Another Automated GC/MS/FID system constructed of pre-concentrator with Varian 3800 GC and Saturn 2200 MS was also deployed to measure VOCs. On each day two samples were collected and measured (8:00-9:00 and 13:00-14:00). To encompass VOCs of a wide range of volatility within each analysis, the system uses dual-columns and dual-detectors to simultaneously analyze both low and high-boiling compounds with each injection. The PLOT column connected to a FID was responsible for separation and detection of C2–C4 compounds, and the DB-1 column was connected to the MS for separation and detection of MTBE and C4–C10 compounds. Each

aliquot of 190 ml from the canisters was drawn to the cryogenic trap packed with fine glass beads cooled at –170 °C for pre-concentration. During injection, the trap was resistively heated up to 80 °C within seconds, and a stream of high purity He flushed the trapped VOCs onto the columns. The oven temperature was initially held at –50 °C for 3.1 min, then ramped to –10 °C at 20 °C/min, to 120 °C at 5 °C/min, to 180 °C at 20 °C/min, and held at 180 °C for 21.5 min. The precision of the system was examined by repeatedly injecting a standard mixture made from Scott Marrin Company. In general, the precision for the C2–C10 NMHCs were usually below 3%. Linearity was tested by trapping a series of the same standard mixture of various concentrations (0.2-30ppbv). Most compounds exhibited good linearity with RSD of calibration response factors for measured species bellow than 10%.

OVOC compounds were measured using a newly developed PFPH-GC/MS method (*S10*). Three types of gaseous carbonyls, including formaldehyde, acetaldehyde and acetone were collected within 3-h sampling period onto an adsorbent (Tenax TA) coated with pentafluorophenyl hydrazine (PFPH) followed by thermal desorption and gas chromatographic (GC) analysis of the PFPH derivatives with mass spectrometric (MS) detection (Agilent, GC/MS, 6890/5973N). All of the tested carbonyls are shown to have method detection limits (MDLs) of sub-nanomoles per sampling tube, corresponding to air concentrations of < 0.3 ppbv for a sampled volume of 24 L. These limits are 2-12 times lower than those that can be obtained using the DNPH/HPLC method (*S10*). The uncertainty for OVOC measurements is estimated to be 10%.

Additional descriptions of the 1-D REAM model

Oxidation mechanism of aromatics. We adopt the aromatics-oxidation mechanism in the SAPRC-07 chemical mechanism developed for chemical transport models (*S14*). This mechanism is chosen because careful comparison between different mechanisms (e.g. SAPRC-99, 07, CB4,

RACM and the mechanism in REAM) indicates that SAPRC-07 mechanism is the most compatible with REAM and reflects the most recent updates of understanding of aromatics chemistry. In Table S1, we summarize the OH reactions for several key aromatic species, based on which the reactions for the lumped species (ARO1, ARO2) are derived. Among the products, only methylglyoxal (MGLY), glyoxal (GLYX), and biacetyl (BACL)) are shown because they are precursors for acetyl peroxy radical, which is of our interest in this work.

Model VOC input. Individual NMHC compounds were lumped into a number of model species to be used as model input. The mean concentrations for all the individual compounds and their corresponding lumped species are shown in Table S2. For species only measured at 8:00–9:00 and 13:00–14:00, interpolations were conducted based on ratios between these compounds and other continuously measured compounds with similar lifetimes.

Estimation of Model errors. The errors associated to the model are estimated as follows. The uncertainty associated with chemical mechanism is estimated to be less than 10% based on a sensitivity test, in which using different chemical mechanisms (RACM or REAM) only results in no more than 10% difference of simulated PAN. The uncertainty associated with transport is estimated to be 10% at most, because 5 times the modeled diffusion coefficient would only result in less than 10% change of PAN at surface. Taking into account all these aspects, the total error in the model is estimated to be no more than 15% assuming transport and chemistry errors are not correlated and not accounting for the measurement uncertainties of precursors.

Integration of production or loss rate and OPE in the planetary boundary layer (PBL)

The hourly average production or loss rate integrated in the PBL is computed using the following equation,

$$\bar{x}^{j} = \frac{\sum_{i} x_i^j \cdot z_i^j}{h_j} \quad \text{(S1)}$$

where i is the layer index, j is hour index, x_i^j is the hourly production or loss rate in layer i and hour j, z_i^j is the hourly thickness of layer i in hour j, and h_j is the hourly PBL height in hour j. Equation (S1) is integrated from the surface to the top of boundary layer during daytime.

The daytime average O_3 production or loss rate integrated in the PBL is integrated to the maximum PBL height, which is the mixing extent of O_3 in the PBL. It is computed using the following equation,

$$\bar{x} = \frac{\sum_{j}\sum_{i} x_i^j \cdot z_i^j}{\sum_{j} h_{\max}} \quad \text{(S2)}$$

where i is the layer index, j is hour index, x_i^j is the hourly production or loss rate in layer i and hour j, z_i^j is the hourly thickness of layer i in hour j, and h_{max} is the maximum hourly PBL height of the day. Equation (S1) is integrated from the surface to the top of the maximum hourly PBL height during daytime.

The daytime average OPE integrated in the PBL is computed similarly,

$$OPE = \frac{\sum_{j}\sum_{i} P(O_3)_i^j \cdot z_i^j}{\sum_{j}\sum_{i} P(NO_z)_i^j \cdot z_i^j} \quad \text{(S3)}$$

where i is the layer index, j is hour index, P_i^j is the hourly production rate of O_3 or NO_z in layer i and hour j, and z_i^j is the hourly thickness of layer i in hour j. Equation (S1) is integrated from the surface to the top of the maximum hourly PBL height during daytime.

Literature Cited

(S1) Ryerson, T. B.; Williams, E. J.; Fehsenfeld, F. C. An efficient photolysis system for fast-response NO_2 measurements. *J. Geophys. Res.-Atmos.*, **2000**, 105, 26447-26461.

(S2) Slusher, D. L.; Huey, L. G.; Tanner, D. J.; Flocke, F. M.; Roberts, J. M. A thermal dissociation-chemical ionization mass spectrometry (TD-CIMS) technique for the simultaneous measurement of peroxyacyl nitrates and dinitrogen pentoxide. *J. Geophys. Res.-Atmos.*, **2004**, *109*, D19315, doi:10.1029/2004JD004670.

(S3) Turnipseed, A. A.; Huey, L.G.; Nemitz, E.; Stickel, R.; Higgs, J.; Tanner, D.; Slusher, D.; Sparks, J.; Flocke F.; Guenther, A. Eddy Covariance Fluxes of Peroxyacetyl Nitrate (PAN) and NO_y to a Coniferous Forest. *J. Gephys. Res.-Atmos.* **2006**, 111, D09304, doi: 10.1029/2005JD006631.

(S4) Flocke, F. M.; Weinheimer, A. J.; Swanson, A. L.; Roberts, J. M.; Schmitt, R.; Shertz, S. On the measurement of PANs by gas chromatography and electron capture detection. *J. Atmos. Chem.*, **2005**, 52, 19-43.

(S5) Amoroso, A.; Beine, H. J.; Sparapani, R.; Nardino, M.; Allegrini, I. Observation of coinciding arctic boundary layer ozone depletion and snow surface emissions of nitrous acid. *Atmos. Environ.*, **2006**, 40, 1949-1956.

(S6) Amoroso, A.; Beine, H. J.; Esposito, G.; Perrino, C.; Catrambone, M.; Allegrini, I. Seasonal differences in atmospheric nitrous acid near Mediterranean urban areas. *Water Air Soil Pollut.*, **2008**, 188, 81-92.

(S7) Febo, A.; Perrino, C.; Cortiello M. A denuder technique for the measurement of nitrous acid in urban atmosphere. *Atmos. Environ.,* **1993***,* 27A, 1721-1728.

(S8) Syomin, D. A.; Finlaysin-Pitt, B. J. HONO decomposition on borosilicate glass surfaces: implications for environmental chamber studies and field experiments. Phy. Chem. Chem. Phys., **2003**, 5, 5236-5242.

(S9) Xie, X; Shao, M.; Liu, Y; Lu, S. H.; Chang, C. C.; Chen, Z. M. Estimate of initial isoprene contribution to ozone formation potential in Beijing, China. *Atmos. Environ.,* **2008***,* 42, 6000-6010.

(S10) Ho, S. S. H.; Yu, J. Z. Determination of airborne carbonyls: Comparison of a thermal desorption/GC method with the standard DNPH/HPLC method. *Environ. Sci. Technol.*, **2004**, 38, 862-870.

(S11) Zhao, C.; Wang, Y. H.; Zeng, T. East China Plains: A "Basin" of Ozone Pollution. *Environ. Sci. Technol.* **2009**, 43, 1911-1915.

(S12) Skamarock, W. C.; klemp, J. B.; Dudhia, J.; Gill, D. O.; Barker, D. M.; Wang, W.; Powers, J. G. A Description of the Advanced Research WRF Version 2. NCAR Tech. Note, June, **2005**.

(S13) Zhao, C.; Wang, Y. H.; Choi, Y.; Zeng T. Summertime impact of convective transport and lightning NOx production over North America: modeling dependence on meteorological simulations. *Atmos. Chem. Phys.*, **2009**, 9, 4315-4327.

(S14) Carter, W. P. L. Development of the SAPRC-07 chemical mechanism and upadated ozone reactivity scales. Final Report to the California Air Resources Board Contract No. 03-318, **2009**.

196 **Tables and figures**

197 **Table S1.** Reactions and rate constants for aromatics species with OH used in SAPRC-07 for deriving the lumped mechanism.

Species	Reactions	k	Mixing ratio (ppbv)	MGLY contribution (%)
Benzene	BENZENE + OH = 0.29 GLYX + Products	1.22E-12	2.2	1
Ethylbenzene	ETHYLBZ + OH = 0.184GLYX + 0.117MGLY + Products	7.00E-12	3.2	4
Toluene	TOLUENE + OH = 0.238 GLY + 0.151 MGLY +Products	5.58E-12	5.9	8
m-Xylene[1]	M-XYLENE + OH = 0.38 MGLY + Products	2.31E-11	2.2	31
o-Xylene	O-XYLENE + OH = 0.238 MGLY + 0.084GLYX + 0.185BACL + Products	1.36E-11	1.7	9
p-Xylene[1]	P-XYLENE + OH = 0.112 MGLY + 0.286GLYX + Products	1.43E-11	2.2	6
1,2,3-Trimethyl Benzene	123TMB + OH = 0.072 MGLY + 0.18GLYX + 0.447BACL+ Products	3.27E-11	0.3	1
1,2,4-Trimethyl Benzene	124TMB + OH = 0.405 MGLY + 0.074GLYX + 0.112BACL+ Products	3.25E-11	0.4	8
1,3,5-Trimethyl Benzene	135TMB + OH = 0.64 MGLY + Products	5.67E-11	0.5	32
ARO1[2]	ARO1 + OH = 0.218 GLYX + 0.138 MGLY + Products	6.15E-12	11.3	15
ARO2[3]	ARO2 + OH = 0.116 GLYX + 0.286 MGLY + 0.104 BACL + Products	2.57E-11	7.3	85

198

199 [1] These two species were measured as one species mp-xylene, and we assume the same amount for each in this calculation.

200 [2] ARO1 includes benzene (×30%), ethyl-benzene, and toluene.

201 [3] ARO2 includes all aromatics other than those included in ARO1.

202 **Table S2.** Average mixing ratios (ppbv) of explicit and lumped NMHCs in the model.

	Alkanes	
C2H6[1]	Ethane[2]	3.82
C3H8	**Propane**[3]	**3.73**
ALK4	**isobutane**	**1.85**
	n-butane	**2.14**
	isopentane	**3.50**
	n-pentane	**1.22**
	2,2-dimthylbutane	0.07
	cyclopentane	0.14
	2-methylpentane	0.69
	3-methylpentane	0.50
	n-hexane	**1.40**
	2,4-dimethylpentane	0.06
	methylcyclopentane	0.47
	cyclohexane	0.18
	2-methylhexane	0.21
	2,3-dimethylpentane	0.09
	3-methylhexane	0.25
	2,2,4-trimethylpentane	**0.47**
	n-heptane	**3.47**
	methylcyclohexane	0.14
	2,3,4-trimethylpentane	0.03
	2-methylheptane	0.09
	3-methylheptane	0.09
	n-octane	**0.91**
	n-nonane	0.11
	Alkyne	
C2H2	ethyne	5.67

	Alkenes	
C2H4	ethene	3.67
PRPE	**Propene**	**1.00**
	trans-2-butene	**0.53**
	1-butene	0.58
	Isobutene	0.37
	cis-2-butene	**0.42**
	3-methyl-1-butene	0.08
	1,3-Butadiene	**0.31**
	1-pentene	**0.57**
	Isoprene	**0.88**
	trans-2-pentene	**0.24**
	cis-2-pentene	0.09
	2-methyl-2-butene	0.18
	Cyclopentene	0.03
	4-methyl-1-pentene	0.00
	2-methyl-1-pentene	0.08
	trans-2-hexene	0.00
	cis-2-hexene	0.04
	alpha-pinene	0.13
	Aromatics	
ARO1	**Benzene**	**2.16**
	Toluene	**5.88**
	Styrene	0.12
	Ethylbenzene	**3.25**
ARO2	**m,p-xylene**	**4.30**
	o-xylene	**1.68**
	Isopropylbenzene	0.04
	n-propylbenzene	0.05
	1,3,5-trimethylbenzene	**0.54**
	1,2,4-trimethylbenzene	**0.37**
	1,2,3-trimethylbenzene	**0.32**

203
204 [1] Model species are listed to the left and measured species are listed to the right. Lumped model
205 species include multiple measured species.
206 [2]Species listed in normal font were measured at 8:00-9:00 and 13:00-14:00 each day; the averages
207 of these measurements are shown.
208 [3]Species listed in bold font were measured continuously each hour; 24-hour averages are shown.
209

Table S3. Daytime (6:00 – 18:00) average mixing ratios (ppbv) of formaldehyde, acetaldehyde, methyl glyoxal and glyoxal from observations and the model S0 and S2 (without aromatics); model values are sampled from the days with observed data.

	Formaldehyde	Acetaldehyde	Methylglyoxal	Glyoxal
Observed	12.4	7.0	0.9	3.1
S0	10.9	6.8	1.0	3.5
S2	4.9	4.1	0.2	0.3

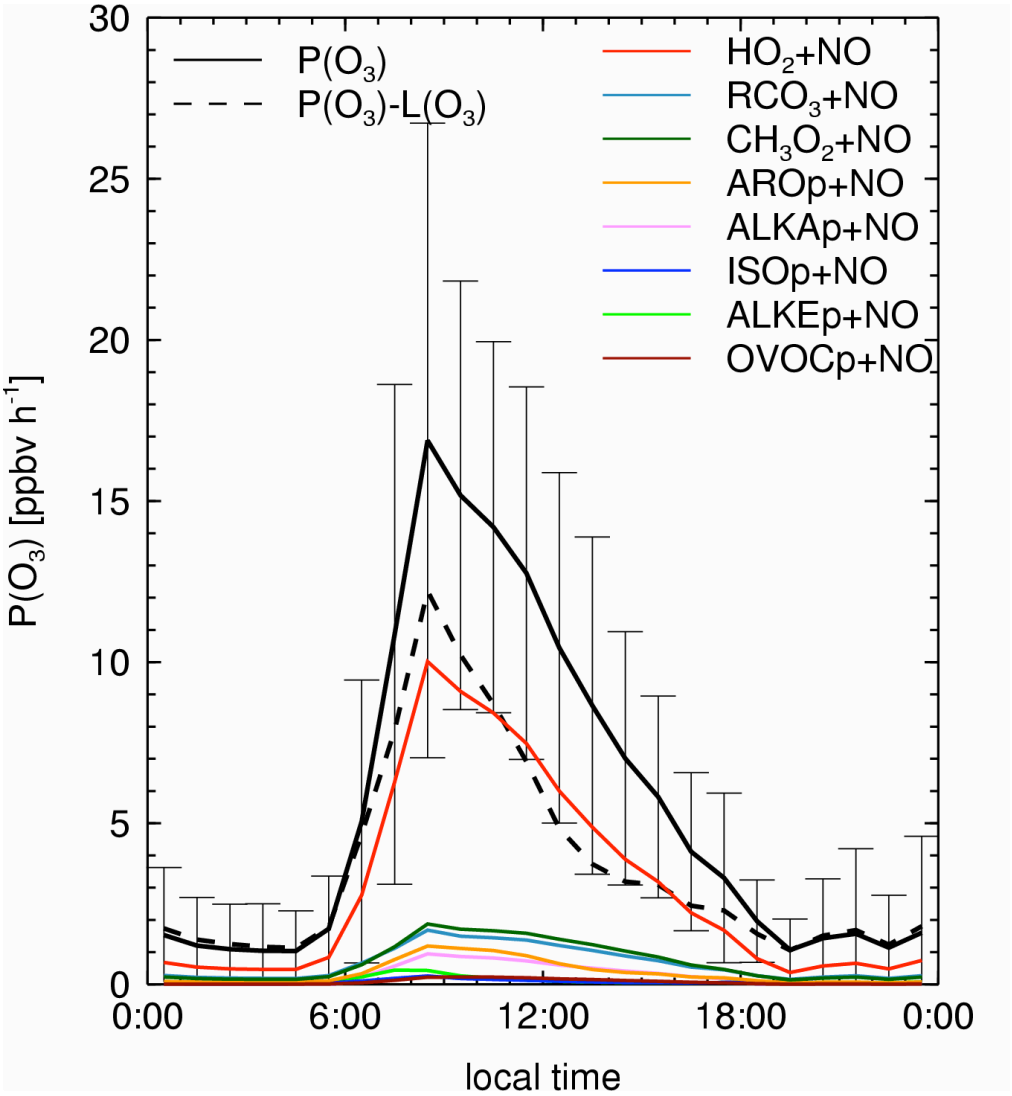

Figure S1. Average diurnal profiles and breakdowns of O_3 production rates (ppbv h^{-1}) integrated in the PBL. The vertical bars show the standard deviation.

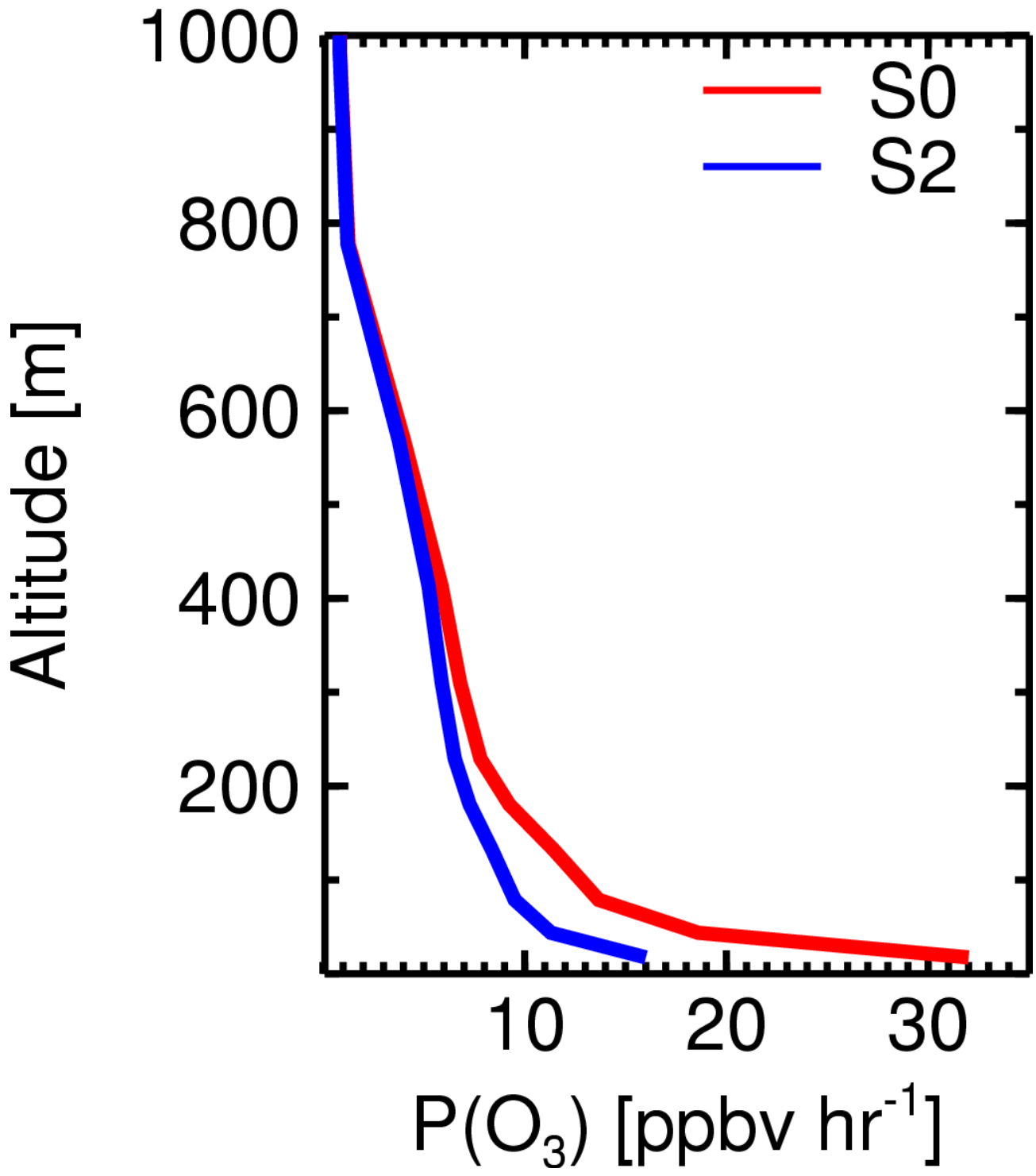

Figure S2. Vertical profiles of daytime averaged vertical distribution of $P(O_3)$ from the surface to 1 km for simulations S0 and S2.

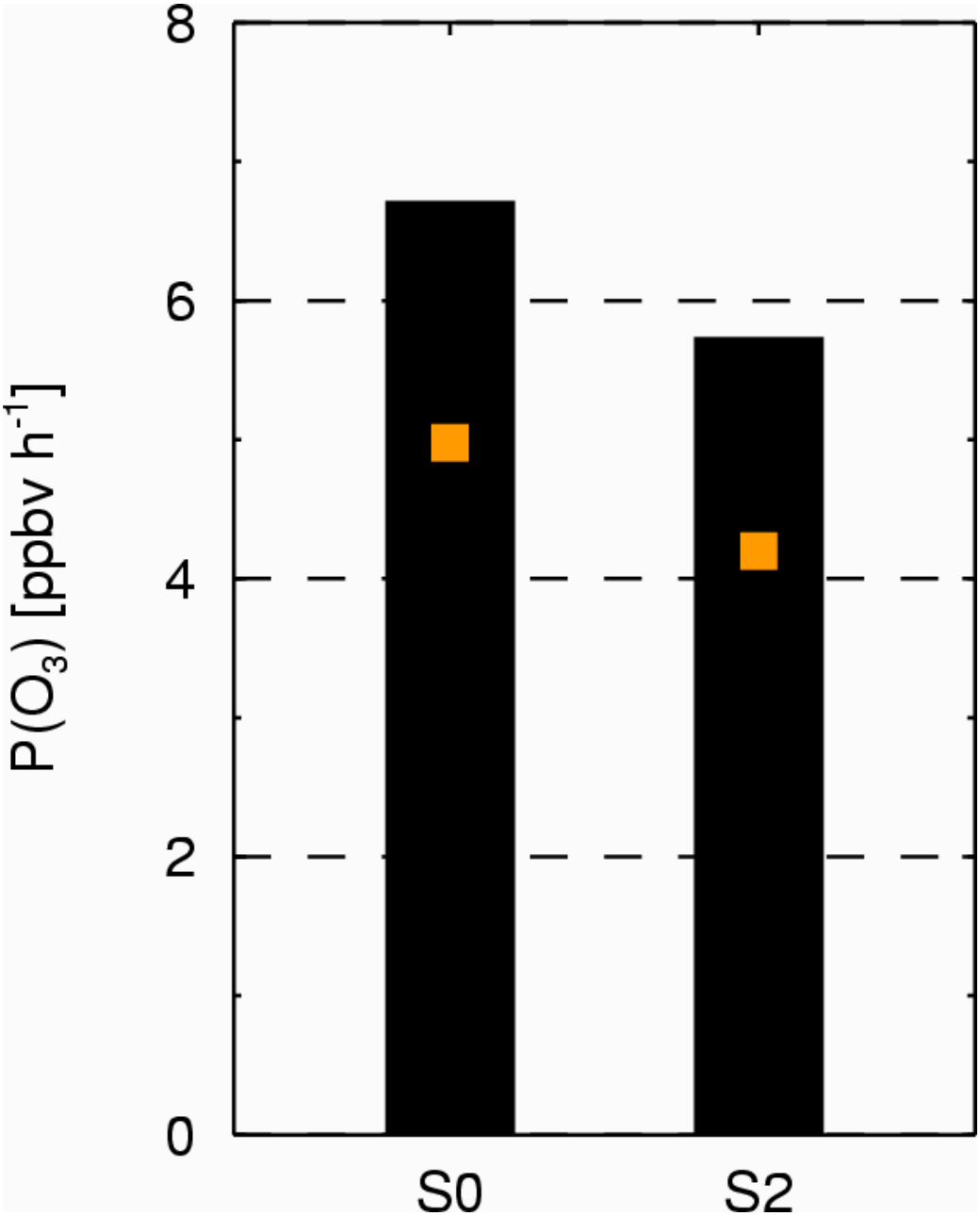

Figure S3. Daytime average O_3 production rates integrated in the PBL under scenarios S0 and S2.

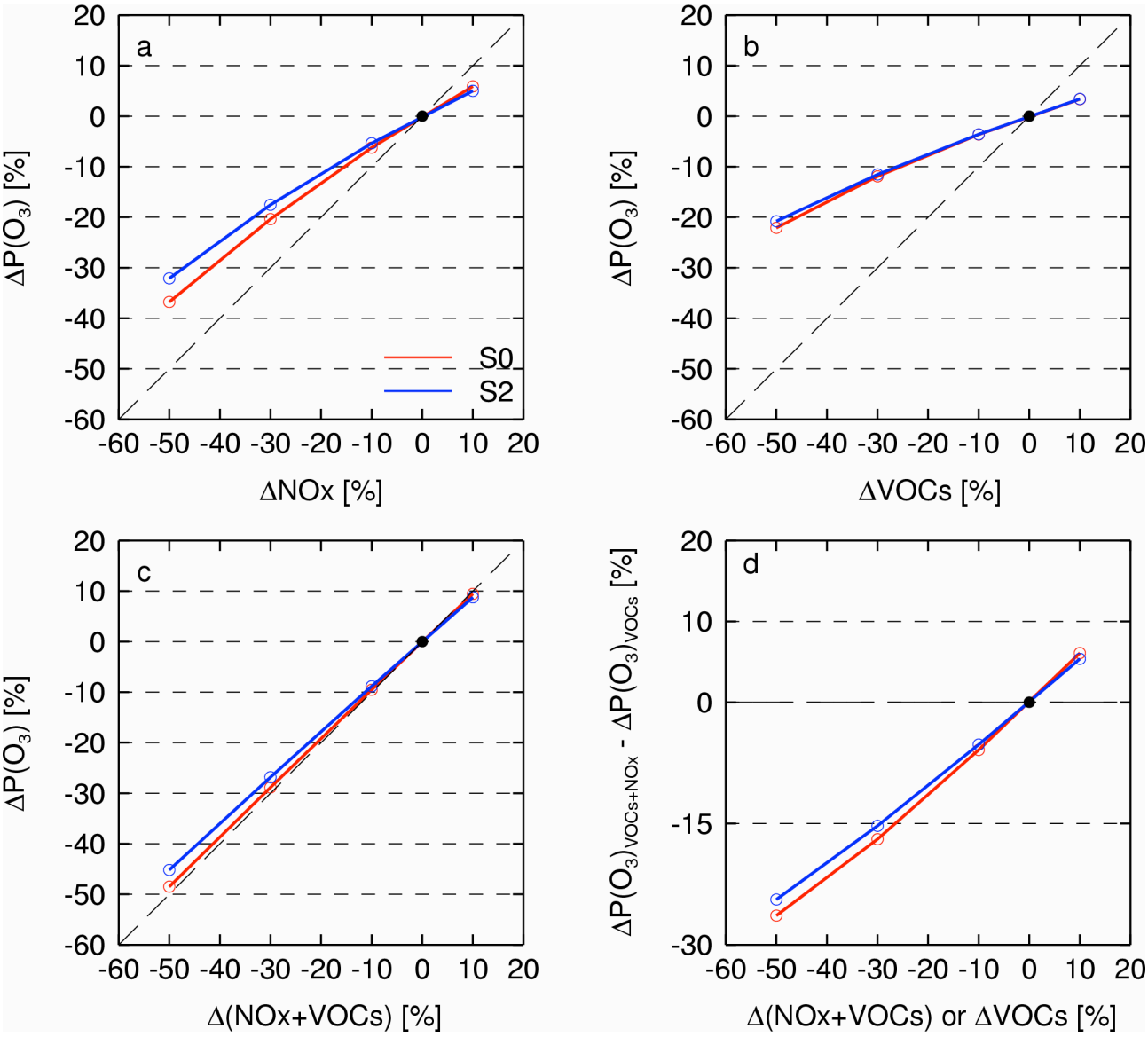

Figure S4. Changes of PBL average O_3 production ($\Delta P(O_3)$) as a function of NOx, VOCs, and both for simulations S0 and S2.

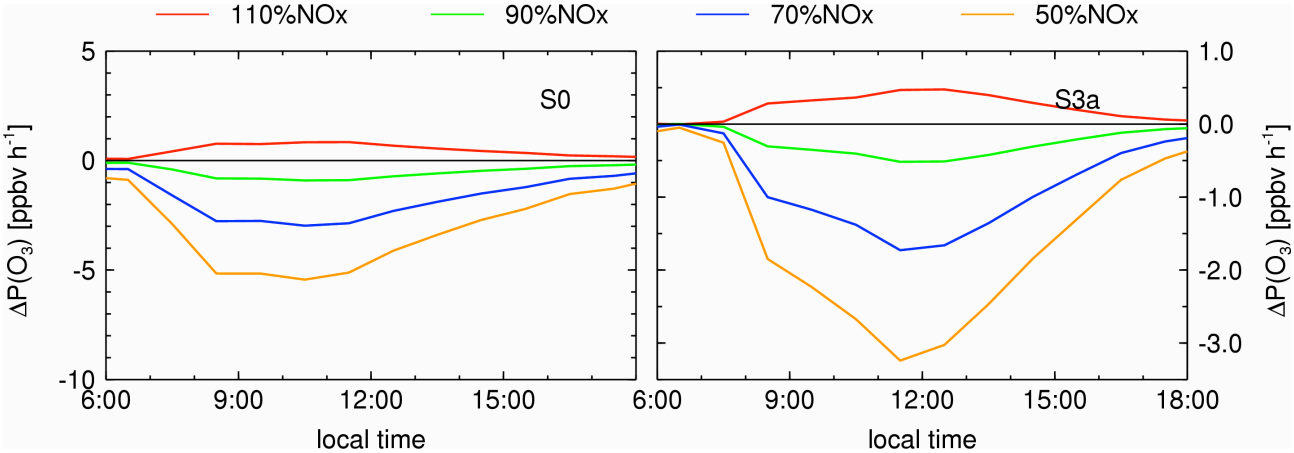

235

236 **Figure S5.** Hourly $\Delta P(O_3)$ integrated in the PBL due to NOx changes under S0 and S3a.

237
238
239
240
241